

An efficient microgrid model based on Markov fuzzy demand-side management

G.K. JABASH SAMUEL¹*, M.S. SIVAGAMA SUNDARI², R. BHAVANI³, and A. JASMINE GNANAMALAR⁴

¹ Department of Electrical and Electronics Engineering, Rohini College of Engineering and Technology, Kanyakumari, India

² Department of Electrical and Electronics Engineering, Amrita College of Engineering and Technology, Nagercoil, India

³ Department of Electrical and Electronics Engineering, Mepco Schlenk Engineering College, Sivakasi-626004, India

⁴ Department of Electrical and Electronics Engineering, PSN College of Engineering and Technology, Anna University, India

Abstract. Today's electricity management mainly focuses on smart grid implementation for better power utilization. Supply-demand balancing, and high operating costs are still considered the most challenging factors in the smart grid. To overcome this drawback, a Markov fuzzy real-time demand-side manager (MARKOV FRDSM) is proposed to reduce the operating cost of the smart grid system and maintain a supply-demand balance in an uncertain environment. In addition, a non-linear model predictive controller (NMPC) is designed to give a global solution to the non-linear optimization problem with real-time requirements based on the uncertainties over the forecasted load demands and current load status. The proposed MARKOV FRDSM provides a faster scale power allocation concerning fuzzy optimization and deals with uncertainties and imprecision. The implemented results show the proposed MARKOV FRDSM model reduces the cost of operation of the microgrid by 1.95%, 1.16%, and 1.09% than the existing method such as differential evolution and real coded genetic algorithm and maintains the supply-demand balance in the microgrid.

Key words: smart grid; non-linear model predictive controller; fuzzy Markov decision process; power scheduling; operating cost.

1. INTRODUCTION

A smart grid is a future power system that combines modern sensor technologies, control techniques, and communication technology at both the transmission and distribution levels to provide electricity in a smart and environmentally beneficial manner [1]. Consumer-friendly poles are the fundamental qualities of a smart grid, self-repairing in a hack-proof mode and resistance to attacks, ability for all forms of storage and generation options, efficient operation on the electricity market, high power quality, and maximum resources [2]. This complex network is guided by various economic, political, social, and technological factors.

Demand-side management is a key role in future smart grid energy management, which supports smart grid functionality in a variety of sectors including electricity market control, infrastructure building, decentralized energy, and electric vehicle management [3, 4]. The creation of an electric network that is under-appreciated in terms of power and transmission will theoretically prevent demand-side management problems.

Demand-side management also performs an important role in the electricity market [5, 6]. A cluster central control system advises on the cluster capabilities for load scheduling and load reduction available for the system. The centralized controller position deals with the market so that certain loads are moved due

to the high demand. Currently, unpredictable as well as changing existing sources of climates such as solar and wind power together with spontaneous consumer habits have brought about major uncertainties in the microgrid system, making it difficult to control MG energy [7, 8]. Demand-side response (DSR) was viewed to function as a source of energy storage or backup power required for the distributed resources. New challenges and possibilities for the fit operation of the MG system are created by the diversified and intelligently designed of DSRs [9]. The DSM development has become an area of significant ongoing research to counter uncertainties and organize DSRs in MG. This research work proposes a Markov fuzzy real-time demand-side manager (MARKOV FRDSM) to minimize the cost of operation of the smart grid system. The obtained simulation result shows that the proposed method reduces the cost of operation of a smart grid by 35% better than the existing methods such as differential evolution, or real coded genetic algorithm, and maintains the supply-demand balance in a smart grid.

This paper is organized as follows: Section 2 gives an overview of the literature survey; the details of the proposed Markov fuzzy real-time demand-side manager are explained in Section 3; in Section 4 the experimental results and analysis are discussed and finally, Section 5 concludes the paper.

2. LITERATURE SURVEY

This section explains various surveys related to the demand-side management system in microgrids studied throughout the years. The present state of production cost and solving the day

*e-mail: jabasamuelgk@gmail.com

Manuscript submitted 2022-06-17, revised 2023-02-14, initially accepted for publication 2023-03-13, published in June 2023.

ahead schedule is discussed, and an overview is provided in this study.

Essiet, *et al.* presented an improved multi-objective DE algorithm (SDE) inspired by the scavenging strategy of hyenas and vultures to minimize the cost in the demand-side management system [10].

Venkatesh *et al.* presented the antlion optimization which minimizes the peak demand and decreases the electricity bills. The load-shifting technique minimizes the demand-side management problem. The results demonstrated that the proposed process generates correct results in terms of electrical energy consumption, as well as supporting the utility of peak load demand and reshaping the demand curve. High-cost operation is a major drawback [11].

Al Salloum *et al.* presented the Stackelberg multi-period multi-provider game the costs and demands for energy are calculated based on a bidirectional communication system between providers and customers. The simulation results revealed that the real-time algorithm is highly efficient and utilizes the least amount of energy. The instability of renewable energy is a drawback [12].

Lizondo *et al.* adapted an artificial immune network algorithm to the peak load problem. The method is especially well-suited to dealing with the peak load problem that arises in tropical and subtropical regions due to the simultaneous use of thousands of these devices. The method was tested on both synthetic and real-world data. As performance measures, the maximal and average tolerance shows that the system keeps the consumption within 1% of the given load [13]. The low performance of multi-level control of the smart grid is the major issue.

Muthukumaran *et al.* presented the elephant herd optimization-based firefly evolutionary algorithm that effectively monitors the real power loss in the smart grid network. The simulation results show that the proposed smart controller for demand-side management reduces power loss and improves the voltage profile significantly. Cost functions are not maintained [14].

Puttamadappa *et al.* presented a combination of glow-worm swarm optimization (GSO) and support vector machine (SVM) employed in the decision-making process in battery storage. The simulation result showed that the suggested method reduces the energy cost and has an average residual load [15].

In Tang *et al.*, the Stackelberg game was based on their identified Nash equilibria, and the grid was optimized to reduce the net profit price and reduce demand fluctuation and also minimize the electricity bills. The results reveal that the proposed fundamental interaction enhanced net profit by 8% and reduced demand variation by roughly 40% for the grid, with 2.5–8.3% savings in electricity bills for the buildings [16]. Furthermore, the robust interaction proposed significantly mitigated the unfavorable impacts of prediction uncertainty.

Bharathi *et al.* [17] presented the genetic algorithm in demand-side management (GA-DSM) was used to find the optimal fitness function of load redistribution in the industry. The result showed that the suggested method solved the issue of power demand reduction, and the flexible load shape is maintained. Cao *et al.* [18] presented the cost-oriented optimiza-

tion methodology for cloud-based information and communication technology that allocates cloud computing resources flexibly. The result showed that the suggested method reduced the operating cost of the cloud platform of demand-side management.

Hashmi *et al.* [19] presented the Internet of Things and cloud computing-based energy management system which generated the load profile of consumers to access remotely. The output displays the consumer load profiles in terms of current, voltage, and power generated. Liu *et al.* [20] presented the scalable and robust demand-side management (SRDSM) approach which minimizes the problem of smart grid operating costs with distributed renewable energy resources. The result showed that the SRDSM algorithm has more scalable and more efficient in size.

Several works consider the difficulties of scheduling, harmonic loss, uncertainties, power imbalance, computational time, cost, and other factors were proposed, none of them is successful in establishing real-time demand-side management, to overcome the above challenges this research proposed a novel Markov fuzzy real-time demand-side management, and its detailed process is presented in next section.

3. PROPOSED MARKOV FUZZY REAL-TIME DEMAND-SIDE MANAGEMENT MODEL

This work is focused on the online demand-side manager for a microgrid. It mainly concentrates on real-time uncertainties rather than forecasting errors of uncertain renewable generation (URG). In this paper, a proposed Markov fuzzy real-time demand-side manager (MARKOV FRDSM) is developed.

The process flow is represented in Fig. 1. It is a two-stage process, with Stage 1 as a fuzzy real-time demand-side manager controller (FRDSM) and Stage 2 as a predictive Markov real-time allocator. Stage 1 is mainly designed for reducing the cost of the operation of the microgrid system and to continue supply and demand must be balanced under a given environment with uncertainties.

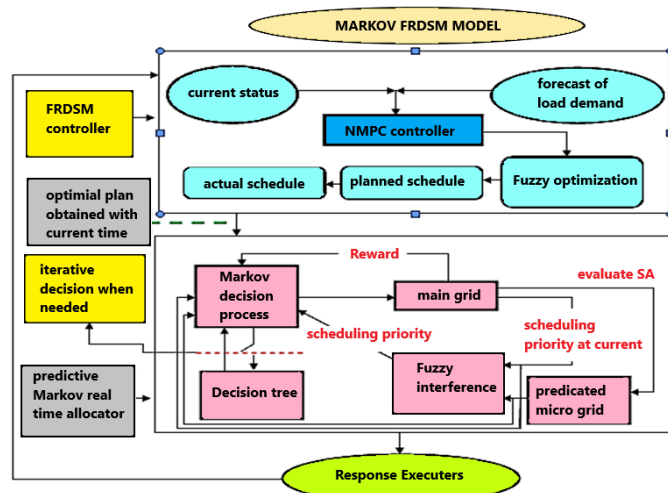


Fig. 1. Block diagram for proposed Markov fuzzy real time demand-side management model

Stage 2 provides a faster scale power allocation concerning fuzzy optimization. Stage 2 is also subdivided into two parts in which the scheduling priority of the response executer is decided by fuzzy interference and the decision-making approach is based on the Markov decision process.

3.1. Fuzzy real-time demand-side manager controller

A fuzzy real-time demand-side manager is proposed for reducing the cost of the microgrid system. NMPC controller gives a global solution to the resulting non-linear optimization problem with real-time requirements based on the uncertainties over the forecasted load demands and current load status. NMPC-based fuzzy optimization mainly aims toward cost minimization of the microgrid. Figure 2 shows the block diagram for NMPC-based fuzzy optimization. The uncertainties framework has difficulties with the ideal activity of the MG, dynamic DSM was developed the counteract these uncertainties.

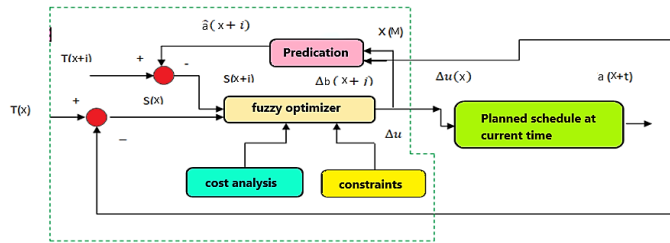


Fig. 2. Block diagram for NMPC-based fuzzy optimization

To manage the dynamic DSM, an NMPC-dependent fuzzy optimization is suggested so that it can make the decisions for the response executers based on the uncertainties within a stage. It has the capability of updating the current status as well as the predicted range of the microgrid (MG).

Let us consider a nonlinear discrete-time state-space model that must be controlled to get an optimal scheduling plan as stated in equations (1) and (2)

$$a(x+1) = f(a(x), b(x)), \quad (1)$$

$$a(x+t) = g(a(x)), \quad (2)$$

where, $a(x) \in R^{n_r \times 1}$, $b(x) \in R^{n_r+t \times 1}$ and $x(r+t) \in R^{n_x \times 1}$ states with the vectors of the corresponding state, control input, and output at sampling time x . f and g state the uncertainties. By increasing the output index, the optimal control sequence is calculated. Often this is a quadratic function that involves future control entries and tracking errors by considering equation (3)

$$e(x+i|x) = a_d(x+i|x) - \hat{a}(x+i|x), \quad (3)$$

where $x_d(x+i|x)$ indicates the reference sequence to be followed that must be known as priori. The cost function 1 is given in the equation

$$quali = \sum_{i=1}^{h_p} \|e(x+i|x)\|_Q^2 + \sum_{j=1}^{h_c} \|b(x+i|x)\|_R^2, \quad (4)$$

where $\|x\|_M^2 = x^T M x$. Q and R defines positive weighing matrices, $Q \geq 0$ and $R \geq 0$. The J minimization is often carried out subject to certain control input constraints and status variables. The limitations can be defined in the following form as stated in equations (5) and (6)

$$\mathbb{U} = \{v \in R^{n_v \times 1} \mid v_{\min} \leq v \leq v_{\max}\}, \quad (5)$$

$$\mathbb{X} = \{x \in R^{n_x \times 1} \mid x_{\min} \leq x \leq x_{\max}\}, \quad (6)$$

v_{\max} , v_{\min} , x_{\max} , x_{\min} are known to be constant vectors. \mathbb{U} and \mathbb{X} are said to be constraint subsets. An NMPC controller aims towards obtaining an output response closest to the referred response such as $[b(x|x), b(x+1|x), \dots, v(r+h_c-1|r)]$. The membership function includes lower and high limits along with a purely monotonous function that decreases continuously.

Incremental fuel costs are not precise, as the cost of fuel may change over time and the type of fuel may be different for each unit. As a result, the membership functions can be used to describe the objective position

$$U_{fi} = \begin{cases} 0 & \text{if } f_i \geq f_{i\max}, \\ \frac{f_{i\max} - f_i}{f_{i\max} - f_{i\min}} & \text{if } f_{i\min} < f_i < f_{i\max}, \\ 1 & \text{if } f_i \leq f_{i\min}, \end{cases} \quad (7)$$

where f_i and $f_{i\max}$ are the minimum and maximum values of the i -th target function, respectively. It is calculated by individually optimizing each target.

3.2. Objective function

The microgrid optimal scheduling problem would commence with the detailed representation of the cost objective function followed by operational constraints of distributed generation (DG) units that are interconnected to the utility. The main objective of this work is to find the best generation set points for DG units in order to reduce total cost when dealing with demand response. Total cost includes DG fuel consumption, unit startup costs, and the market price for a power exchange between the MG and the grid. The following equations express the objective functions and constraints of the proposed work.

$$\begin{aligned} \min F(\gamma) &= \sum_{x=1}^X X C^x \\ &= \sum_{x=1}^X \left\{ \sum_{i=1}^{NG} [v_i^x A_{DGi}^x S_{DGi}^x + U_{DGi} |V_i^x - V_i^{x-1}|] \right. \\ &\quad \left. + \sum_{j=1}^{NS} [v_j^x A_{ESj}^x S_{ESj}^x + U_{ESj} |V_j^x - V_j^{x-1}|] + A_{vx}^x S_{grid}^x \right\}, \quad (8) \end{aligned}$$

$$\gamma = \begin{bmatrix} A_{DG1}^x, A_{DG2}^x, \dots, A_{NG}^x, A_{ES1}^x, A_{ES2}^x, \dots, A_{NS}^x, A_{vx}^x, \\ v_1^x, v_2^x, \dots, v_{NG+NS}^x \end{bmatrix}, \quad (9)$$

The vector denotes γ decision variables such as the active power of the i th DG unit and the j -th storage unit, as well as their ON/OFF states. Equation (8) shows the cost operating formula.

$S_{DG_i}^x$ and $S_{ES_j}^x$ are the bids of DG and storage units at hour x , A_{vx}^x is the active power exchange from/to utility at hour x , and S_{grid}^x is the utility bid cost at hour x .

Power balance. The active power balancing constraint is one of the most essential constraints in the EMS problem since it ensures that the total active power generated by the DG units, BESS, and utility is sufficient to meet the overall load demand.

$$\sum_{i=1}^x A_{DG_i}^x + \sum_{j=1}^x A_{ES_j}^x + A_{vx}^x = \sum_{x=1}^x A_{load}^x. \quad (10)$$

Uncertain load constraints. In real-time, there is no crisp load; the load value changes every minute. For load demand, all load demands are assumed to be fluid in nature and can be expressed via Gaussian distribution. As Fig. 3 shows, Q_d never will be less than Q_i or greater than Q_i . This is the best Q_d estimate. In this proposed work, the Gaussian membership function is used. The degree of satisfaction is stated by $\mu_{Q_d} Q_i$ which represents the membership function w.r.t to the i -th constraint and $Q_d + 1$ is the maximum tolerable error in the forecasted peak loads.

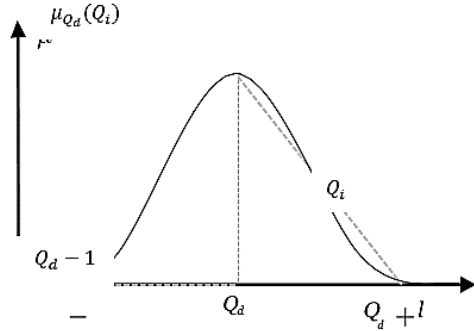


Fig. 3. Gaussian membership functions for load demand

Response executer constraints. The constraint of the RE is stated as follows in equations (8), (9), and (10)

$$T_{j,k} = \frac{S_{j,k-1} + (v_{j,k} P_{j,k} - (1 - v_{j,k}) P_{j,k}) \eta_{j,k}^p \Delta t}{Q_j^{\text{nom}}}, \quad (11)$$

$$S_j^{\text{min}} \leq S_{j,k} \leq S_j^{\text{max}}, \quad (12)$$

$$\begin{cases} 0 \leq P_{j,k} \leq P_j^c, & v_{j,k} = 1, \\ 0 \leq P_{j,k} \leq P_j^d, & v_{j,k} = 0, \end{cases} \quad (13)$$

$$S_i^{\text{ini}} + \frac{\sum_{K \in \mathcal{K}} (v_{j,k} P_{j,k} - (1 - v_{j,k}) P_{j,k}) \eta_{j,k}^p \Delta t}{Q_j^{\text{nom}}} \geq S_j^E, \quad \forall j \leq n. \quad (14)$$

Power charging and discharging at all times, as specified in (12); S_j^{min} and S_j^{max} indicate RE_j minimum and maximum allowable SOC levels, respectively; Q_j^{nom} indicates RE_j battery capacity. $\eta_{j,k}^p$ represents the efficiency of power exchange, $\eta_{j,k}^p = \eta_j^c$, $v_{i,k} = 1$ and $\eta_{j,k}^p = 1/\eta_j^d$ with $v_{j,k} = 0$, where η_j^d and η_j^c represents charging as well as discharging.

3.3. Predictive Markov real-time power allocator

Markov decision process (MDP) provides a decision-based result for the allocated plan based on the current time under a stochastic environment an agent is required to take action in order to attain a goal [21]. The decision-making process mainly takes place under the shorter sampling period T_s so as to activate an action within a state $a \in s$ which is defined as a policy $\varphi: s \rightarrow a$. Additionally, to obtain an optimal policy the time samples were divided further into sub-steps ζ with an ΔT and $k_t \in \{1, 2, \dots, \zeta\}$ at any step-in time. Point a vigorous sequential for the corresponding action using a dynamic programming equation that is iteratively solved to provide an optimal solution. This process is combined with the scheduling plan that was obtained in Stage 1.

Initially, the power compensation at the time step is calculated for MG. P_{kj}^{tot} is obtained by equation (15)

$$P_{kj}^{\text{tot}} = P_{kt}^{\text{WT}} + P_{kt}^{\text{PV}} - L_{kt}^B, \quad (15)$$

where P_{kt}^{WT} , P_{kt}^{PV} and L_{kt}^B states an output of windmill, solar, and load demand. Based on the overall power compensation the MDP decides the compensation state at time t ,

$$\begin{cases} \phi^{V2G}(P_{kt}^{\text{tot}}) = \begin{cases} 1, & P_{kt}^{\text{tot}} < 0, \\ 0, & P_{kt}^{\text{tot}} \geq 0, \end{cases} \\ \phi^{G2V}(P_{kt}^{\text{tot}}) = \begin{cases} 0, & P_{kt}^{\text{tot}} < 0, \\ 1, & P_{kt}^{\text{tot}} \geq 0, \end{cases} \end{cases} \quad (16)$$

where ϕ^{V2G} and ϕ^{G2V} represents a vehicle-to-grid and grid-to-vehicle compensation state, respectively

$$\phi^{V2G}(P_{kt}^{\text{tot}}) \cdot \phi^{G2V}(P_{kt}^{\text{tot}}) = 0.$$

Space of the state. The power compensation is believed to be known to the operator. We describe the state space as the sum of the WT and PV system on moving state information centered on the MG. And each phase is built on a horizon of prediction.

Transition and recompense functions. Transition and recompense functions are provided below. The transition functions are established in relation to the WT and PV state quantities, and fuzzy threat estimation determines the entries. The sampling time is increased in the sum changed with $M + 1 = M + \Delta(M)$. The likelihood entries are updated based on WT and PV state quantity, at a given status value

$$T(s(k+1), a(k), s(k)) = \begin{cases} 1 - \mathcal{L}_{ij}(k), & \text{transiting a SA,} \\ \mathcal{L}_{ij}(k), & \text{studying in SA,} \end{cases} \quad (17)$$

where the logistic weight is $\mathcal{L}_{ij}(k)$, i.e., with a logistic feature axis in mind that only one scheduling ability change is considered, and if once the SA is fixed by the MDP then it can be changed based on RE feedback, or can remain in the same

SA [22]. Reward function based on the correct SA is defined in the following way

$$\mathfrak{R}(s(M+1), a(M), s(M)) = o_1 \mathfrak{D}_{ij}(k) + o_2 \mathfrak{F}_{ij}(k), \quad (18)$$

where o_1 and o_2 are the user feature, \mathfrak{D}_{ij} is the long-term secure space, and \mathfrak{F}_{ij} is the scheduling capability.

Fuzzy optimization is described as

$$S_{j,k}^* = S_{i,k}^{\text{ini}} + \frac{\sum_{k'}^k \left(v_{j,k}^* P_{j,k'}^* - (1 - v_{j,k}^*) P_{j,k'}^* \right) \eta_{j,k'}^p, \Delta t}{Q_i^{\text{nom}}}, \quad (19)$$

where $P_{j,k}^*$ and $v_{j,k}^*$ are the first stage yielded the scheduling plan and the status of RE_i at time step k , respectively.

Utility of agent system for scheduling ability. The REs have different abilities to reduce the power balance using MG technology due to a different online status (for example, payment level and needed energy in the current stage) and background information.

Our work shows that REs can manage the imbalance of power based on the SA concept, and we provide an assessment system to determine SA values based on the online status of each RE as well as the history of each RE. The assessment indices we are going to consider are:

Insufficient storage. $P_{kt}^{\text{com}} > 0$ insufficient storage states cannot store the excess power that may be generated RE and cannot absorb that which causes the problem of imbalance even though consisting of excess power. Thus, the power storage lag was expressed as

$$I_S^1 = Q^{G2V} (P_{kt}^{\text{tot}}) \frac{P_f^c \eta^c (\Delta t - k_t \Delta T)}{Q_i^{\text{nom}} (s_j^* - s_{ik_t} - 1)}. \quad (20)$$

where I_S^2 express the insufficient storage.

Irregular supply. $P_{kt}^{\text{tot}} < 0$ means that URG generations cannot meet the MG demand for the load. In other words, MG requires V2 G energy. The REs must therefore discharge its stored energy in order to satisfy the MG compensation requirement. An RE that is very keen to pay will usually be very reluctant to unlock it. Thus, the capacity of the power supply index and the charging urgent level index are mutually interrelated. The REI power supply capacity can then be defined as

$$I_S^2 = Q^{G2V} (P_{kt}^{\text{tot}}) \frac{P_f^c \eta^c (\Delta t - k_t \Delta T) - Q_i^{\text{nom}} (s_j^* - s_{ik_t} - 1)}{P_f^c \eta^c (\Delta t - k_t \Delta T)}. \quad (21)$$

Online prediction loss. $P_{kt}^{\text{tot}+} \leq 0$ states that during online demand management, there may be a chance of uncertainties which may cause energy loss as well as load imbalance. Uncertainties such as environmental disasters, charge-discharge problems of batteries, and the depth of discharge may lead to inefficient management by the RE as well as MG. Online prediction

loss is expressed by

$$I_S^{3+} = Q^{G2V} (P_{kt}^{\text{tot}}) \frac{\sum_{k'} \left(v_{j,k}^* P_{j,k'}^* - (1 - v_{j,k}^*) P_{j,k'}^* \right) \eta_{j,k'}^p, \Delta t}{Q_i^{\text{nom}}}. \quad (22)$$

3.4. Fuzzy interference-based schedule priority

Fuzzy interference provides optimal schedule priority (policy) to the MDP to decide on it. A fuzzy interference provides control over the decision made by the MDP on schedule priority. Consider the fuzzy system evolving the transition matrix $P_{j,k}^* = [P_{S(1)}^T, \dots, P_{S(n)}^T]$, where $P_{S(1)}^T$ states the row vector representing a fuzzy transition under the action of I_S^n . Therefore, the initial fuzzy transition for state $S^{(0)}$ is given by

$$S^t = S^0 o P(P_{j,k}^0) o P(P_{j,k}^1) o \dots o P(P_{j,k}^{t-1}). \quad (23)$$

Now the major role of MDP is to reach the goal set by fuzzy, which is $g = \{g(1), \dots, g(n)\}$ where g states the optimal value to maximize the following quantity

$$S^* o g \rightarrow w.r.t. \left[P_{j,k}^0, \dots, P_{j,k}^{(t-1)*} \right], \quad (24)$$

where S is a transition state, t^* is the number of steps in which the scheduled plan on the prior base should be achieved.

4. RESULT AND DISCUSSION

This section illustrates the result analysis of different operation modes taken in the proposed demand-supply model. The simulation analyzed different load-shifting points under optimal scheduling. The net load calculation of real-time DSM is evaluated under different uncertainties. The real-time scenario from two household electricity utilization and financial saving is derived under MARKOV FRDSM scheduling technique. The proposed MARKOV FRDSM scheduling technique is compared with the existing algorithms such as differential evolution (DE) [10] and real-coded genetic algorithm [17].

4.1. Load shifting using optimal scheduling

Residential electricity using the two previously indicated scheduling methods in an uncoordinated charging framework is analyzed. Based on their electricity usage trends, electricity customers were divided into clusters like Household 1 and Household 2. The power habits of two houses from two nearby clusters are depicted in Fig. 4.

The highest-priority electrical loads in the house must be met first, according to a fuzzy interference-based policy. Household 1 is scheduled ahead of Household 2 in the proposed MARKOV FRDSM. The electricity supplier has changed both the provided power usage patterns by Household 1 and Household 2 as displayed in Fig. 5. The electricity provider will move the customer power use to different times. As an outcome of fuzzy scheduling, the degree of shifted electricity for each timeslot is shown in Fig. 6. When compared to Household 1, it can be seen that Household 2 has the majority of loads moved. In fact, Household 1 received 91.2% of the power. As a result,

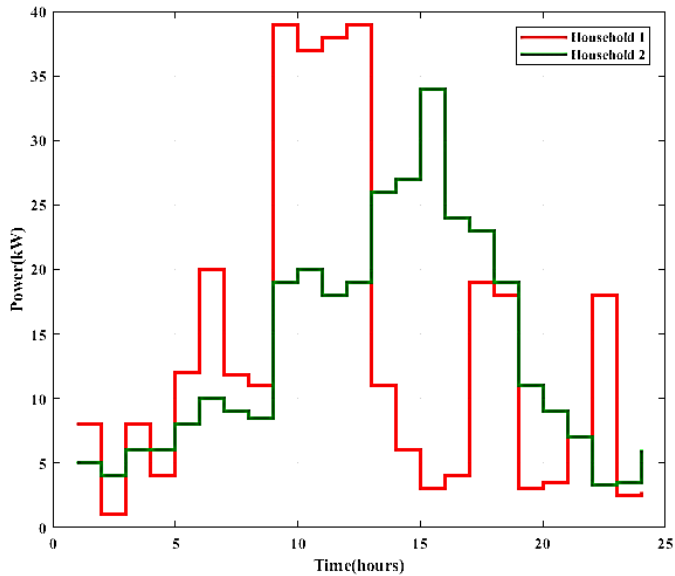


Fig. 4. A sample of load consumption profiles from two households

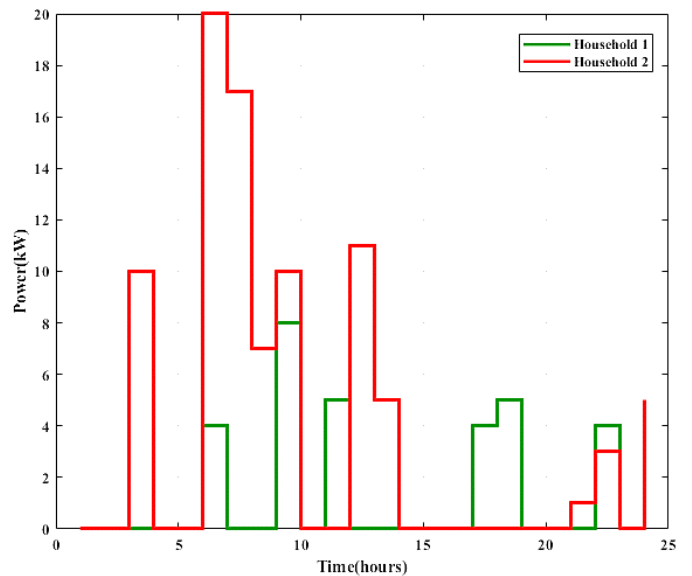


Fig. 6. Electricity demand shifts as a result of the FCFS policy

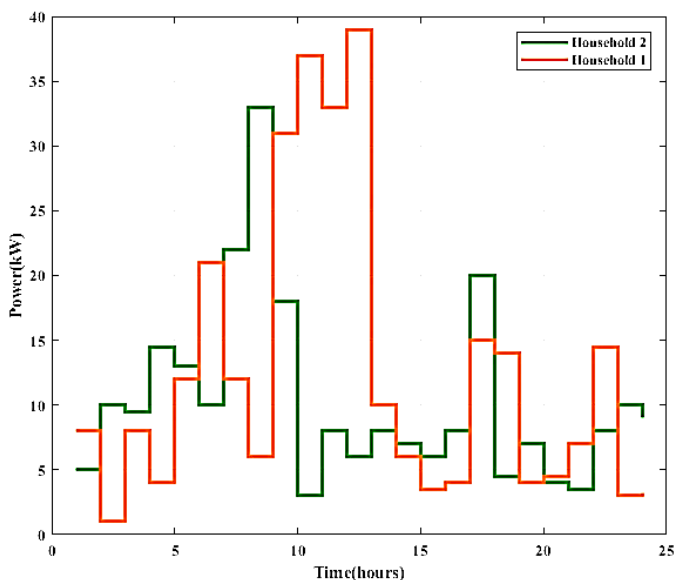


Fig. 5. Modified electricity profile with FCFS policy

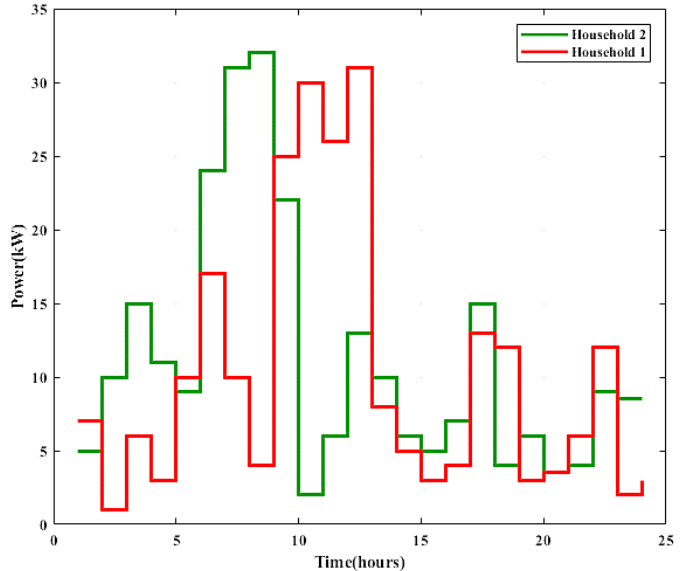


Fig. 7. Power supply profile for two households realized with fuzzy Markov scheduling policy

8.8% of the load was moved. However, Household 2 electrical demand was altered significantly with 73.9% of its targeted power usage scheduled being implemented.

Furthermore, comparison of two household financial savings on power bills demonstrates that Household 1 saves far more than Household 2. Household 1 used to have a savings rate of 24.57%, whereas Household 2 had a savings rate of 17.10%. The fuzzy Markov scheduling policy seeks to handle the level of shifting electricity demand associated with fuzzy interference by ensuring electricity to all appliances in order to offset the enormous gap in financial savings amongst customers. The new power supply profiles of two households created with the fuzzy Markov scheduling approach are shown in Fig. 7. Figure 8 also shows the degree of shifting client loads. As a result

of this, Fig. 9 depicts the overall load demands and the output of the URGs under the four control techniques described previously.

Figure 10 depicts the system net loads for uncoordinated control (UC), real-time demand-side management (RDSM) without real-time power allocation (RTAC), RDSM with RTAC, and real-time control (RTC) techniques. The characteristics of the system net load, such as the peak-valley difference, the fluctuation rate, and the relative peak reduction (RPR) [15] were clearly enhanced after considering the optimum scheduling of the REs in the later three techniques, as shown in Fig. 10. In particular, the suggested RDSM with RTAC outperforms existing approaches in terms of improving the system net load characteristics.

An efficient microgrid model based on Markov fuzzy demand-side management

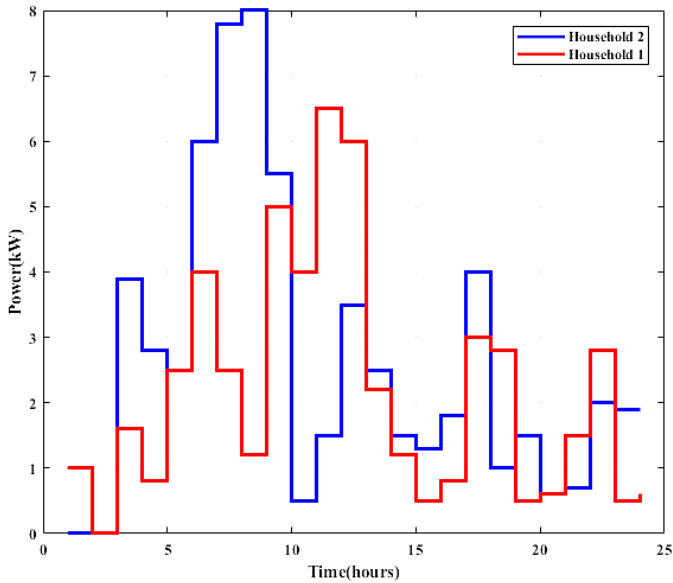


Fig. 8. Modified power profile with AF policy

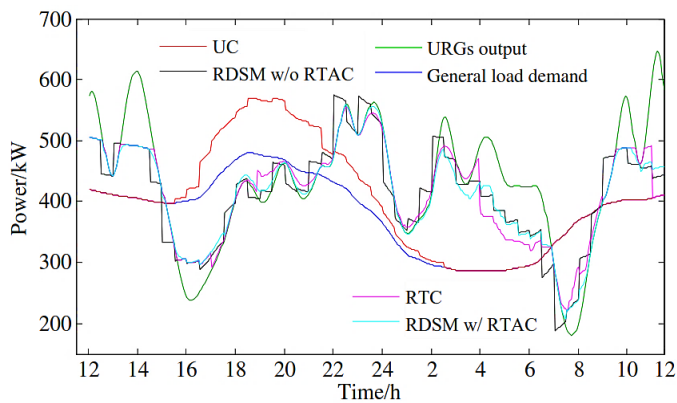


Fig. 9. Curves showing total load under four approaches and the output of the URG

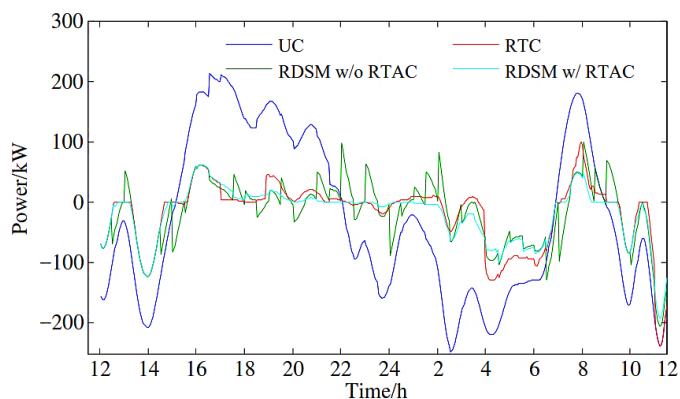


Fig. 10. Curves of system net load under four different ways

The RTC method is intended for MGs on a smaller scale. It is difficult to properly analyze the realistic expression of the charging and discharging urgency level and power allocation

due to its limited operating mechanism. As a result, the RTC methodology has a lower ability to respond to system compensation needs than the fuzzy Markov RDSM method.

Table 1
Microgrid operating cost

Algorithm	Operating cost (%)
Differential Evolution [10]	1.95%
Real Coded Genetic Algorithm [17]	1.16%
Proposed MARKOV FRDSM	1.09%

According to Fig. 11, the proposed MARKOV FRDSM method takes less time (56 seconds) to solve this problem.

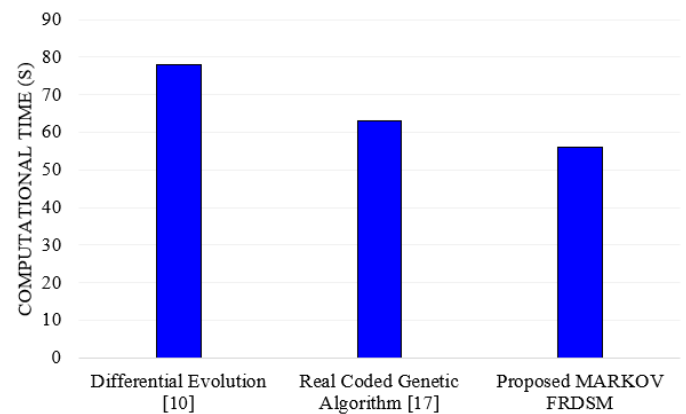


Fig. 11. Comparative analysis of computational time

This is less time when compared with the existing technique as described in the literature [10, 14]. The operation cost of the proposed and existing is evaluated from equation 8 in this analysis. The proposed MARKOV FRDSM reduces the cost of operation of the microgrid which is shown in Table 1. The proposed MARKOV FRDSM t is compared to popular state-of-the-art algorithms like differential evolution (DE) and real-coded genetic algorithms to demonstrate its efficacy.

5. CONCLUSIONS

In this research, a two-stage MARKOV FRDSM that can concentrate on real-time uncertainties is proposed. It mainly consists of two stages. The first stage provides a minimized operation cost as well as maintains a supply-demand balance under uncertain situations. Moreover, it provides an optimal plan for the current time. In the second stage based on the plan, it provides a priority-wise decision to obtain a schedule for allocating the power according to their demand. In addition, a non-linear model predictive controller (NMPC) is designed to give a global solution to the non-linear optimization problem with real-time requirements based on the uncertainties over the forecasted load demands and current load status. Finally, the proposed work was tested on a random basis under various energy

usage, resulting in lower home appliance electricity bills. The overall cost reduction of the microgrid differential evolution, real coded genetic algorithm, and proposed MARKOV FRDSM are 1.95%, 1.16%, and 1.09%, respectively without demand-side management participation.

ACKNOWLEDGEMENTS

The Author with a deep sense of gratitude would thank the supervisor for his guidance and constant support rendered during this research.

REFERENCES

- [1] Q. Li and M. Zhou, "The future-oriented grid-smart grid," *J. Comput.*, vol. 6, no. 1, pp. 98–105, 2011, doi: [10.4304/jcp.6.1.98-105](https://doi.org/10.4304/jcp.6.1.98-105).
- [2] P. Agrawal, "Overview of DOE microgrid activities," in *Proc. Symp. Microgrid*, 2006, pp. 1–32.
- [3] S. Rahman and Rinaldy, "An efficient load model for analyzing demand side management impacts," *IEEE Trans. Power Syst.*, vol. 8, no. 3, pp. 1219–1226, 1993, doi: [10.1109/59.260874](https://doi.org/10.1109/59.260874).
- [4] I. Cohen and C.C. Wang, "An optimization method for load management scheduling," *IEEE Trans. Power Syst.*, vol. 3, no. 2, pp. 612–618, 1988, doi: [10.1109/59.192913](https://doi.org/10.1109/59.192913).
- [5] M. Shahidehpour, H. Yamin, and Z. Li, *Market Operations in Electric Power Systems: Forecasting, Scheduling, and Risk Management*, New York: Wiley–IEEE Press, 2002, pp. 1–509.
- [6] Z.N. Popovic and D.S. Popovic, "Direct load control as a market-based program in deregulated power industries," in *2003 IEEE Bologna Power Tech Conference Proceedings*, Italy, 2003, p. 4, doi: [10.1109/PTC.2003.1304491](https://doi.org/10.1109/PTC.2003.1304491).
- [7] Z. Zhang, J. Wang, T. Ding, and X. Wang, "A two-layer model for microgrid real-time dispatch based on energy storage system charging/discharging hidden costs," *IEEE Trans. Sustain. Energy*, vol. 8, no. 1, pp. 33–42, 2017, doi: [10.1109/TSTE.2016.2577040](https://doi.org/10.1109/TSTE.2016.2577040).
- [8] H. Yang *et al.*, "Operational planning of electric vehicles for balancing wind power and load fluctuations in a microgrid," *IEEE Trans. Sustain. Energy*, vol. 8, no. 2, pp. 592–604, 2017, doi: [10.1109/TSTE.2016.2613941](https://doi.org/10.1109/TSTE.2016.2613941).
- [9] Rabiee, M. Sadeghi, J. Aghaeic, and A. Heidari, "Optimal operation of microgrids through simultaneous scheduling of electrical vehicles and responsive loads considering wind and PV units uncertainties," *Renew. Sustain. Energy Rev.*, vol. 57, pp. 721–739, 2016, doi: [10.1016/j.rser.2015.12.041](https://doi.org/10.1016/j.rser.2015.12.041).
- [10] I. Essiet, Y. Sun, and Z. Wang, "Scavenging differential evolution algorithm for smart grid demand side management," *Procedia Manuf.*, vol. 35, pp. 595–600, 2019, doi: [10.1016/j.promfg.2019.05.084](https://doi.org/10.1016/j.promfg.2019.05.084).
- [11] S. Ramchurn, P. Vytelingum, A. Rogers, and N. Jennings, "Agent-based control for decentralized demand side management in the smart grid," in *Proc. The 10th International Conference on Autonomous Agents and Multiagent Systems*, Taiwan, 2011, pp. 5–12.
- [12] S. Bu and F.R. Yu, "A game-theoretical scheme in the smart grid with demand-side management: Towards a smart cyber-physical power infrastructure," *IEEE Trans. Emerg. Top. Comput.*, vol. 1, no. 1, pp. 22–32, 2013, doi: [10.1109/TETC.2013.2273457](https://doi.org/10.1109/TETC.2013.2273457).
- [13] Z.M. Fadlullah, D.M. Quan, N. Kato, and I. Stojmenovic, "GTES: An Optimized Game-Theoretic Demand-Side Management Scheme for Smart Grid," *IEEE Syst. J.*, vol. 8, no. 2, pp. 588–597, 2014, doi: [10.1109/JSYST.2013.2260934](https://doi.org/10.1109/JSYST.2013.2260934).
- [14] T. Logenthiran, D. Srinivasan, and T.Z. Shun, "Demand side management in smart grid using heuristic optimization," *IEEE Trans. Smart Grid*, vol. 3, no. 3, pp. 1244–1252, 2012, doi: [10.1109/TSG.2012.2195686](https://doi.org/10.1109/TSG.2012.2195686).
- [15] Z. Zhu, J. Tang, S. Lambotharan, W.H. Chin and Z. Fan, "An integer linear programming-based optimization for home demand-side management in smart grid," in *Proc. 2012 IEEE PES Innovative Smart Grid Technologies (ISGT)*, USA, 2012, pp. 1–5, doi: [10.1109/ISGT.2012.6175785](https://doi.org/10.1109/ISGT.2012.6175785).
- [16] Q. Zhu, Z. Han, and T. Başar, "A differential game approach to distributed demand side management in smart grid," in *Proc. 2012 IEEE International Conference on Communications (ICC)*, Canada, 2012, pp. 3345–3350, doi: [10.1109/ICC.2012.6364562](https://doi.org/10.1109/ICC.2012.6364562).
- [17] C. Bharathi, D. Rekha, and V. Vijayakumar, "Genetic algorithm-based demand side management for smart grid," *Wireless Pers. Commun.*, vol. 93, no. 2, pp. 481–502, 2017, doi: [10.1007/s11277-017-3959-z](https://doi.org/10.1007/s11277-017-3959-z).
- [18] Z. Cao *et al.*, "Optimal cloud computing resource allocation for demand side management in smart grid," *IEEE Trans. Smart Grid*, vol. 8, no. 4, pp. 1943–1955, 2016, doi: [10.1109/TSG.2015.2512712](https://doi.org/10.1109/TSG.2015.2512712).
- [19] S.A. Hashmi, C.F. Ali, and S. Zafar, "Internet of things and cloud computing-based energy management system for demand side management in smart grid," *Int. J. Energy Res.*, vol. 45, no. 1, pp. 1007–1022, 2021, doi: [10.1002/er.6141](https://doi.org/10.1002/er.6141).
- [20] R.S. Liu and Y.F. Hsu, "A scalable and robust approach to demand side management for smart grids with uncertain renewable power generation and bi-directional energy trading," *Int. J. Electr. Power Energy Syst.*, vol. 97, pp. 396–407, 2018, doi: [10.1016/j.ijepes.2017.11.023](https://doi.org/10.1016/j.ijepes.2017.11.023).
- [21] W. Kamrat, "Selected information technology tools supporting maintenance and operation management electrical grids," *Bull. Pol. Acad. Sci. Tech. Sci.*, vol. 69, no. 5, p. e138089, 2021, doi: [10.24425/bpasts.2021.138089](https://doi.org/10.24425/bpasts.2021.138089).
- [22] W. Jarzyna, "A survey of the synchronization process of synchronous generators and power electronic converters," *Bull. Pol. Acad. Sci. Tech. Sci.*, vol. 67, no. 6, pp. 1069–1083, 2019, doi: [10.24425/bpasts.2019.131565](https://doi.org/10.24425/bpasts.2019.131565).